Research Article

Yousef Murtaja, Lubomír Lapčík*, Harun Sepetcioglu, Jakub Vlček, Barbora Lapčíková, Martin Ovsík, and Michal Staněk

Enhancement of the mechanical properties of HDPE mineral nanocomposites by filler particles modulation of the matrix plastic/elastic behavior

Abstract: Two different nanosized mineral fillers (nano calcium carbonate and nanoclay) were used in the high density poly(ethylene) (HDPE) composites pilot plant production. Structural and mechanical properties of the prepared composites were examined in this study. The homogenous filler distribution was confirmed in the tested samples by scanning electron microscopy, transmission electron microscopy, and energy dispersive spectroscopy analyses. The fillers' fortifying effect on polymer composites' mechanical performance was confirmed as indicated by the increased elastic modulus and indentation modulus. Additionally, the possible modulation of the plastic-elastic mechanical behavior was confirmed by the type of the filler as well as its concentration used in the final composites testing articles.

Keywords: nanosized mineral fillers, HDPE, composites, mechanical properties

---

* **Corresponding author: Lubomír Lapčík,** Department of Physical Chemistry, Faculty of Science, Palacky University, 17. Listopadu 12, 771 46 Olomouc, Czech Republic; Department of Food Technology, Faculty of Technology, Tomas Bata University in Zlin, Nam. T.G. Masaryka 275, 760 01 Zlin, Czech Republic, e-mail: lapcikl@seznam.cz
Yousef Murtaja, Jakub Vlček: Department of Physical Chemistry, Faculty of Science, Palacky University, 17. Listopadu 12, 771 46 Olomouc, Czech Republic
Harun Sepetcioglu: Department of Metallurgy and Materials Engineering, Selçuk University, Faculty of Technology, Konya 42075, Turkey
Barbora Lapčíková: Department of Physical Chemistry, Faculty of Science, Palacky University, 17. Listopadu 12, 771 46 Olomouc, Czech Republic; Department of Food Technology, Faculty of Technology, Tomas Bata University in Zlin, Nam. T.G. Masaryka 275, 760 01 Zlin, Czech Republic
Martin Ovsík, Michal Staněk: Department of Manufacturing Technology, Faculty of Technology, Tomas Bata University in Zlin, Nam. T.G. Masaryka 275, 760 01 Zlin, Czech Republic

1 Introduction

The study of the effect of the nano/microsized mineral fillers blended in the high density poly(ethylene) (HDPE) composite matrix on the mechanical properties of the prepared composites gained excessive attraction in the past 10 years due to their wide application in automotive, aerospace industries [1,2], formulation engineering [3], sound damping materials [4], highly conductive polymeric nano-composites [5], dielectric material applications [6], etc. Semi-crystalline polymers exhibit, in general, a free-phase continuum system with the crystalline and amorphous phases separated with interphase. The crystalline part is formed with mutually connected spherulites consisting of crystalline lamellae dispersed in the amorphous phase [7]. The type, shape, and size of the mineral filler have a strong impact on the mechanical properties of the thermoplastic-polymer-based composites as well as on their melting behavior and crystallization kinetics [8]. Furthermore, the nature and the quality of the mutual adhesion between the filler and the polymer matrix [9], filler particle size, shape, and particle size distribution have a paramount effect on the final composite application performance [10,11]. This study offers the mechanical testing of the composites prepared from the commercial fillers compounded with HDPE in industrial-scale semi-pilot conditions. The main aim was to confirm the large-scale processability and reproducibility of the manufacturing steps during composites production.

2 Materials

HDPE of HD8100M grade used in our entire experiment was supplied by Polymer Marketing Company Limited (Thailand). The density of the resin was $0.952\,\text{g/cm}^3$ with a melt flow index of 0.25 g/10 min. The nano calcium carbonate ($CaCO_3$) particles, also known as adaCAL-N1-C,
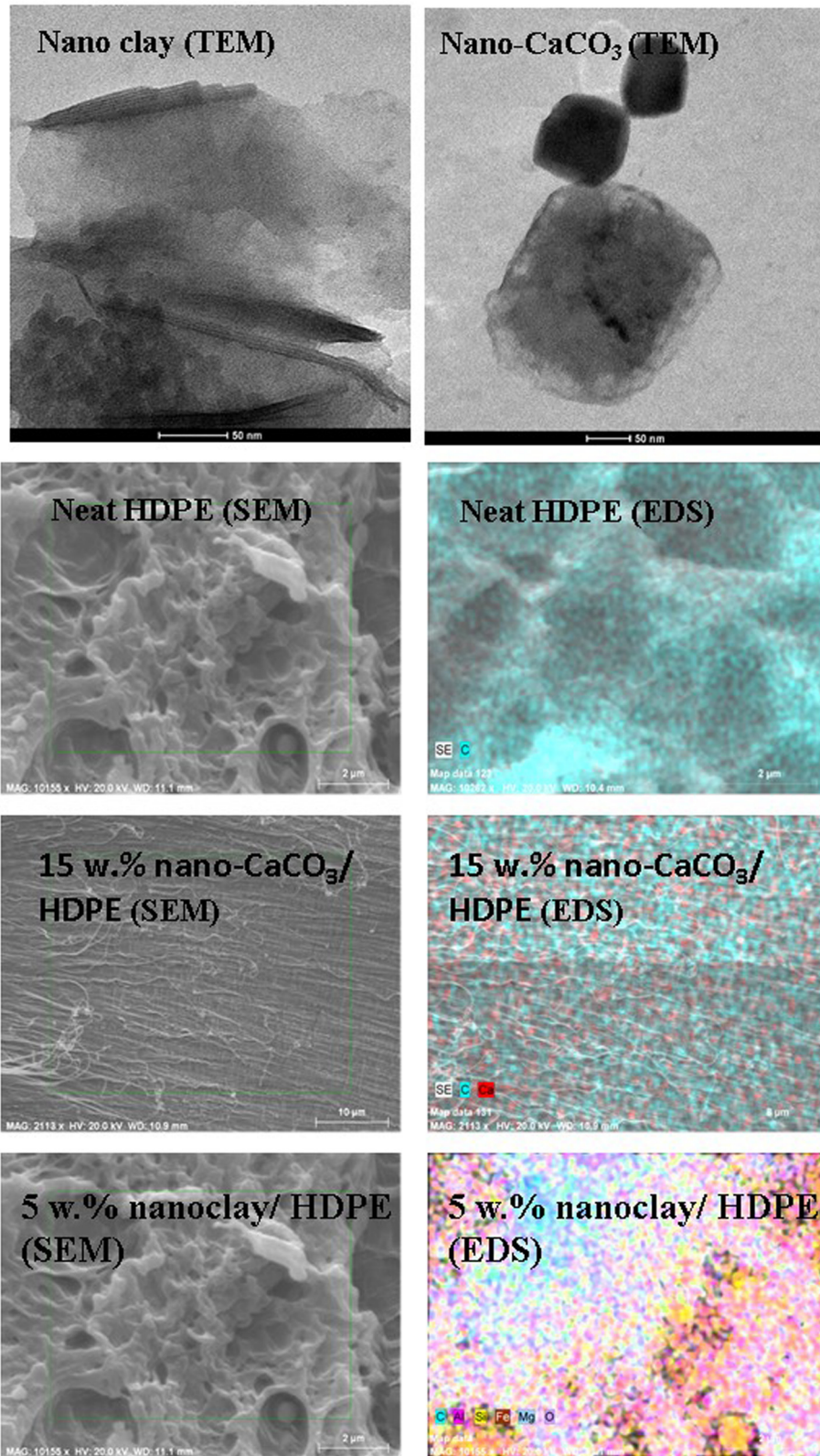
Figure 1: TEM images of the fillers used in this study: Nanoclay and nano CaCO₃.

were received from Adacal Co. (Turkey) and were treated with stearic acid prior to further processing. Particles' average size d_{50} was of 0.05 μm as obtained from scanning electron microscopy (SEM) measurements. Nanoclay particles (i.e., EsanNANO 1-140) were supplied by EczacıbasıEsan (Turkey). Particles' average size d_{50} was of 2.7 μm as obtained from laser diffractometer measurements. SEM and transmission electron microscopy (TEM) images of the prepared samples showed that the nanofillers were homogeneously dispersed within the HDPE matrix (Figure 1). This fact was confirmed also by the energy dispersive spectroscopy (EDS) mapping study.

The chemical compositions and physical properties of the used nano calcium carbonate as well as that of the nanoclay are given in Table 1 and are also available in refs [12,13].

Images of both fillers captured by TEM are shown in Figure 1. For testing, the set of samples of different filler concentrations were prepared and labelled as CC for nano calcium carbonate and NC for nanoclay.

Nanoclay/HDPE nanocomposites were prepared by melt mixing system composed of Banbury mixer, single screw extruder, and granule cutting unit allowing semi-pilot production in 100 kg scale. The processing temperature in the mixer was kept at 180°C and the temperature was reached in 15 min after filling the mixer chamber with both the HDPE granules and the filler [14]. The apparatus was then followed by the extruder with a conveyor belt and the cutting unit. Single screw extruder was operating at 330 rpm screw speed with five barrel temperature profiles of 200, 190, 190, 190, and 220°C. Nanoclay/HDPE nanocomposite hot mixtures were cut in water into the shape of granules. Then, they were molded as tensile and impact test specimens using a PS40E5ASE injection molding machine with a melt temperature of 210°C, mold temperature of 65°C, and injection pressure of 50 MPa [14]. Similarly, the nano CaCO$_3$/HDPE nanocomposites were prepared by the melt mixing method as well by use of the same compounder system and the processing parameters as mentioned above in the case of nanoclay/HDPE composites preparation. For both fillers, the weight ratios of the HDPE and the fillers were maintained to obtain the samples of the given filler weight concentration such as 1, 3, 5, 10, and 15 wt% for CC/HDPE composites and 1, 2, 3, 4, and 5 wt% for NC/HDPE composites.

Millipore water (USA) with a conductivity of 0.06 μS/cm, ethylene glycol p.a., (Lach-Ner, Czechia), and 99%

pure diiodomethane of ACS reagent grade (Sigma Aldrich, Germany) were used as wetting liquids for contact angle measurements.

3 Methods

3.1 SEM and TEM

TEM (FEI Tecnai G2 Spirit Biotwin model, FEI Company, USA) was used to characterize the shape and morphology of the filler particles. TEM images were taken by placing nanofiller samples on a standard 400 grid copper mesh. Dispersions of acetone fillers were ultrasonicated for 15 min and were casted on the copper mesh and air dried. TEM measurements were performed at 120 kV accelerating voltage. Nano CaCO$_3$ and nanoclay's distributions in HDPE matrix were analyzed by TEM. An ultra-thin section of about 100 nm thickness were cut from filled samples using a microtome device (CM1950) supplied by Leica Microsystems Inc. (Buffalo Grove, USA) in a low-temperature environment. For further examination of the distribution of nanofillers, the composites were characterized by SEM using a Zeiss EvoLS10 equipped with an energy-dispersive X-ray detector (Germany).

3.2 Thermal analysis

Differential scanning calorimetry (DSC) experiments were performed according to ASTM E1356 by using a TA Instrument S10 model (Waters, USA) at a nitrogen flow rate of 50 mL/min. Virgin HDPE and its nanocomposites' glass transition temperatures (T_g) were determined from DSC curves by means of the midpoint method at 10°C/min heating rate from 30 to 300°C [13,15].

3.3 Uniaxial tensile testing

Universal Testing Machine Autograph AGS-100 Shimadzu (Japan) and Zwick 1456 multipurpose tester (Germany) equipped with Compact Thermostatic Chamber TCE Series were used for tensile testing of injection-molded specimens.

Table 1: Physicochemical properties of applied fillers: nanoclay and nano CaCO$_3$

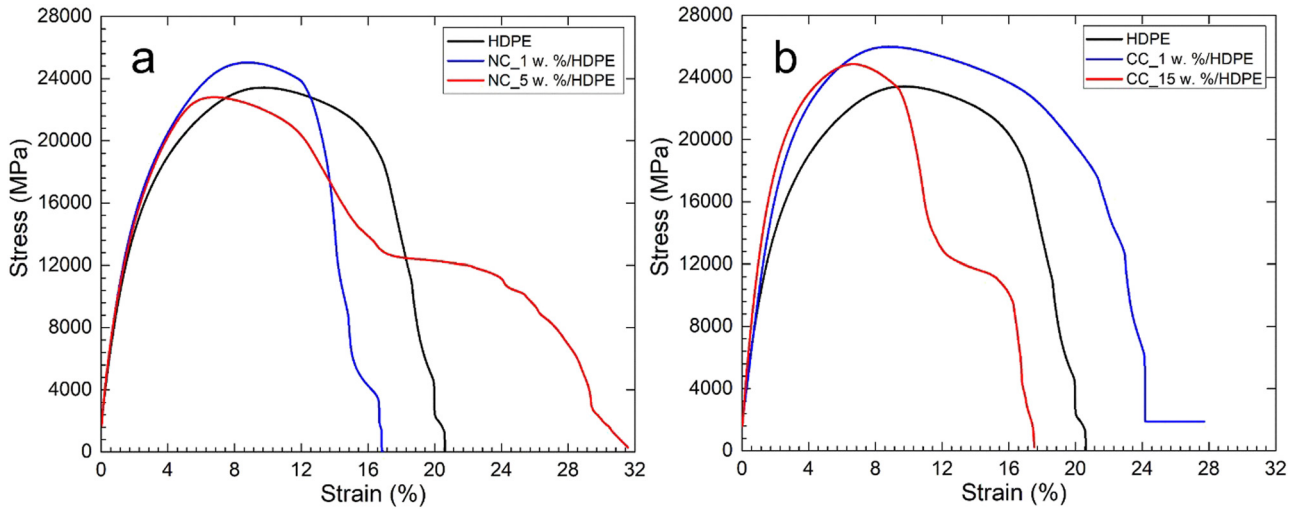| Filler type	Color	Density (g/cm^3)	Surface area (g/m^2)	Particle size (μm)
Nanoclay	Ultra white	1.98	19	2–20
Nano CaCO$_3$	Ultra white	2.95	28	0.05–0.10

Figure 2: (a) General mechanical behavior of NC/HDPE and (b) CC/HDPE composites with different filler concentrations from tensile testing experiments as obtained for 50 mm/min deformation rates at ambient temperature expressed as stress vs strain dependencies.

All data ptwere recorded as per CSN EN ISO 527-1 and CSN EN ISO 527-2 standards taking the tested gauge length of 8 cm. All experiments were performed at room temperature up to break with 50, 100, and 200 mm/min deformation rates. Strength at break, Young's modulus, and strain at break were obtained from the stress-strain dependence plot(s). Each experiment was repeated 10×, and the mean values and standard deviations were calculated. All experiments were performed at the laboratory ambient conditions of 25°C temperature.

3.4 Charpy impact testing

Impact tests were carried out using Zwick 513 Pendulum Impact Tester (Germany) according to the CSN EN ISO

179-2 standard, allowing 25 J energy drop. Each experiment was repeated 10×, and the mean values and standard deviations were calculated. All experiments were performed at the laboratory ambient conditions of 25°C temperature.

3.5 Surface free energy (SFE) characterization

The SFE of the studied composites and pure HDPE was determined by the static contact angle of wetting measurements based on axisymmetric drop shape analysis. All measurements were performed at 23°C and repeated
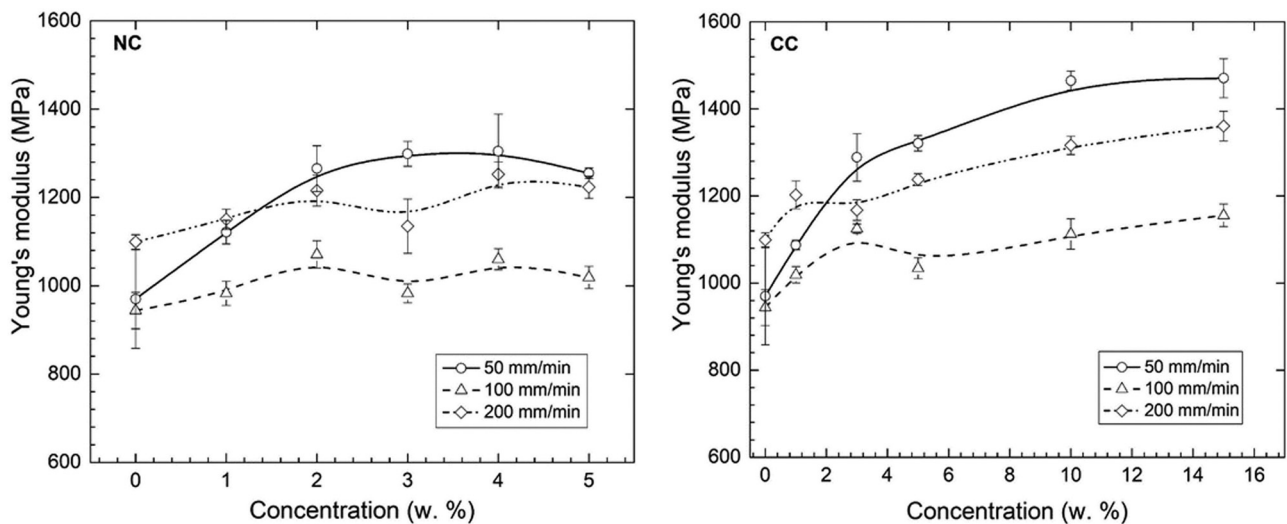

Figure 3: Young's modulus and filler concentration dependencies of the CC/HDPE and NC/HDPE composites obtained with tensile testing experiments for different deformation rates.

Table 2: Results of the tensile testing experiments of the studied HDPE composites at 50, 100, and 200 mm/min deformation rates. Filler concentrations indicated in the sample description are given in wt%

Sample	Young's modulus (MPa) Rate (mm/min)			Upper yield (MPa) Rate (mm/min)			Strain at break (%) Rate (mm/min)			Fracture toughness (kJ/m²)
	50	100	200	50	100	200	50	100	200	
HDPE	970.1 ± 111.7	943.8 ± 142.2	1,099.2 ± 16.2	24.5 ± 1.1	24.8 ± 1.1	25.6 ± 0.4	20.5 ± 0.1	25.8 ± 5.0	16.6 ± 0.6	36.69 ± 5.15
CC_1%	837.5 ± 10.8	648.2 ± 419	1,202.7 ± 32.1	25.4 ± 0.6	24.3 ± 1.1	25.1 ± 0.5	30.8 ± 3.1	33.2 ± 6.7	19.8 ± 0.3	31.48 ± 2.43
CC_3%	1,288.9 ± 54.7	1,368 ± 2.5	1,167.7 ± 23.7	24.4 ± 0.4	25.0 ± 0.2	24.7 ± 0.8	22.0 ± 0.8	19.8 ± 1.0	22.9 ± 1.5	17.26 ± 0.92
CC_5%	1,322 ± 10.8	1,034.3 ± 299	1,237.9 ± 13.7	23.6 ± 0.5	25.4 ± 3.4	25.0 ± 1.1	25.0 ± 3.0	28.5 ± 14.7	17.2 ± 3.1	26.29 ± 1.04
CC_10%	1,465.1 ± 12.3	1,112.8 ± 273	1,316.4 ± 0.4	24.3 ± 1.3	25.2 ± 1.0	26.3 ± 0.7	18.6 ± 2.3	20.5 ± 7.4	14.1 ± 0.4	28.69 ± 3.4
CC_15%	1,470 ± 54.7	1155 ± 255	1,360.7 ± 1.7	24.6 ± 0.2	25.3 ± 1.1	28.1 ± 2.8	20.1 ± 2.6	19.7 ± 6.9	11.2 ± 2.2	31.79 ± 3.94
NC_1%	1,121.4 ± 26.8	982.9 ± 217	1,150.5 ± 23.0	23.6 ± 1.5	26.5 ± 0.5	27.4 ± 2.4	32.8 ± 15.9	19.3 ± 4.6	16.4 ± 6.0	29.21 ± 2.21
NC_2%	1,265.4 ± 51.9	1,070.9 ± 303	1,215.6 ± 48.8	25.8 ± 3.2	27.4 ± 2.2	30.0 ± 2.8	21.2 ± 8.7	20.5 ± 10.5	12.1 ± 0.6	24.37 ± 1.0
NC_3%	1,248.7 ± 28.1	982.7 ± 213	1,134.9 ± 61.2	27.3 ± 1.9	23.9 ± 1.6	22.4 ± 0.4	19.8 ± 3.2	31.1 ± 11.2	26.6 ± 2.2	28.44 ± 0.09
NC_4%	1,304.9 ± 83.7	1,060.1 ± 240	1,328.3 ± 78.0	23.3 ± 0.1	23.9 ± 0.3	27.9 ± 2.5	27.6 ± 2.2	35.7 ± 7.2	14.4 ± 5.9	23.35 ± 0.27
NC_5%	1,255 ± 11.9	1,018.8 ± 246	1,223.3 ± 25.0	23 ± 0.2	23.5 ± 0.2	24.7 ± 0.2	28.9 ± 2.7	32.88 ± 10	20.5 ± 2.1	22.06 ± 1.42

7× with a Krüss DSA 30 (Krüss, Germany). The Owens, Wendt, Rabel, and Kaelble extended Fowkes theory was used to calculate the SFE of the tested composites and pure HDPE from the average static contact angles for water, ethylene glycol, and diiodomethane [16,17].

3.6 Micro hardness

Micro-indentation tests were performed on a micro-indentation tester (Micro Combi Tester, Anton Paar, Austria), according to the CSN EN ISO 14577 standard. The applied diamond tip was of the cube corner shape (Vickers, Anton Paar, Austria). Measurement parameters were set as follows: maximum load of 3 N, loading rate (unloading rate) of 6 N/min, and holding time of 90 s. All experiments were performed according to the depth-sensing indentation method, allowing simultaneous measurement of the acting force on the indentor and the displacement of the indentor's tip. The indentation hardness (H_{IT}) was calculated as the maximum load (F_{max}) on the projected area of the hardness impression (A_p). Indentation modulus (E_{IT}) was calculated from the plane strain modulus of elasticity ($E^\star$) using an estimated Poisson's ratio (v) of the samples (0.3–0.4 [18,19]):

$$H_{IT} = \frac{F_{max}}{A_p}, \tag{1}$$

$$E_{IT} = E^\star(1 - v^2). \tag{2}$$

Each measurement was repeated 10×, and mean values and standard deviations were calculated. All experiments were performed at the laboratory ambient conditions of 25°C temperature.

4 Results and discussion

Results of the tensile testing experiments of the studied composites are shown in Figure 2. Obtained stress vs strain deformation dependencies exhibited typical patterns corresponding to the elastic region (does not exceed 3% strain for small deformations), elastic-plastic transition region (does not exceed 10% strain for small deformations), and the stress plateau draw region occurred for 5 wt% nanoclay/HDPE composites and 15 wt% for CC/HDPE composites at strains exceeding 18% (NC/HDPE composites) and 12% (CC/HDPE composites), respectively [20]. Similar dependencies were found in our previous studies for industrial HDPE mineral composites at the same deformation rate [13,15]. Pure HDPE
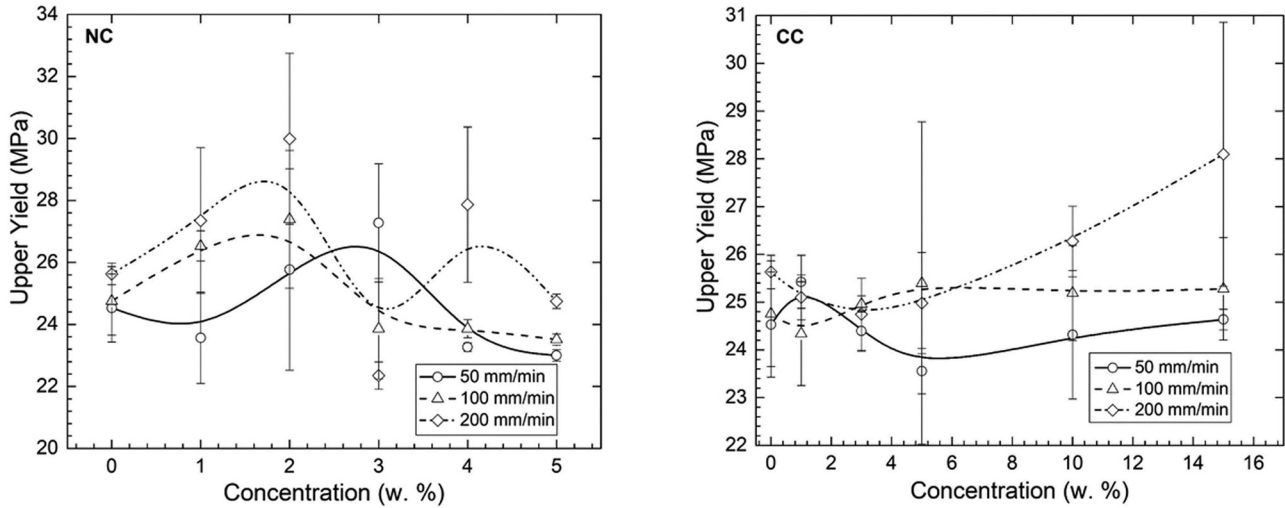
Figure 4: Upper yield and filler concentration dependencies of the CC/HDPE and NC/HDPE composites obtained with tensile testing experiments for different deformation rates.
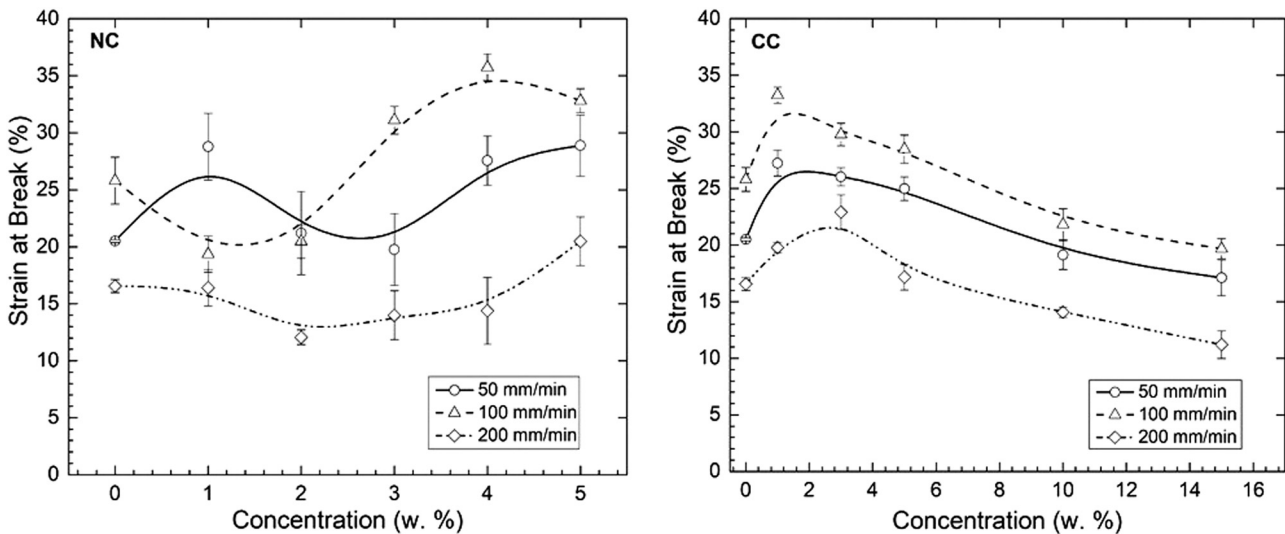

Figure 5: Strain at break and filler concentration dependencies of the CC/HDPE and NC/HDPE composites obtained with tensile testing experiments for different deformation rates.

exhibited more stiff tensile deformation behavior in the absence of the stress plateau draw region. In contrary to that CC/HDPE composites, were characteristic of more elasto-plastic behavior as reflected for 1 wt% filler concentration (Figure 1b). In the case of NC/HDPE composites, there is a significant influence of elastic-plastic properties. With increasing filler concentration, greater plastic behavior was observed, as reflected by the increased stress plateau draw region, as shown in Figure 2b. The abovementioned behavior was also accompanied by the corresponding increase in the Young's modulus of elasticity with increasing filler concentration

for both mineral fillers, as shown in Figure 3. Such behavior was confirmed for all applied deformation rates, as given in Table 2. For example, the absolute value of the modulus of elasticity of 970.1 ± 111.7 MPa for original HDPE was increased to 1470.0 ± 54.7 MPa by about 51.5% in the case of CC/HDPE composites with 5 wt% filler concentration. For the NC/HDPE composites, the modulus E was increased by about 34.5% to the absolute value of 1304.9 ± 83.7 MPa with 4 wt% filler concentration. These corresponded very well with previously published data that stiff mineral filler particles were responsible for the observed
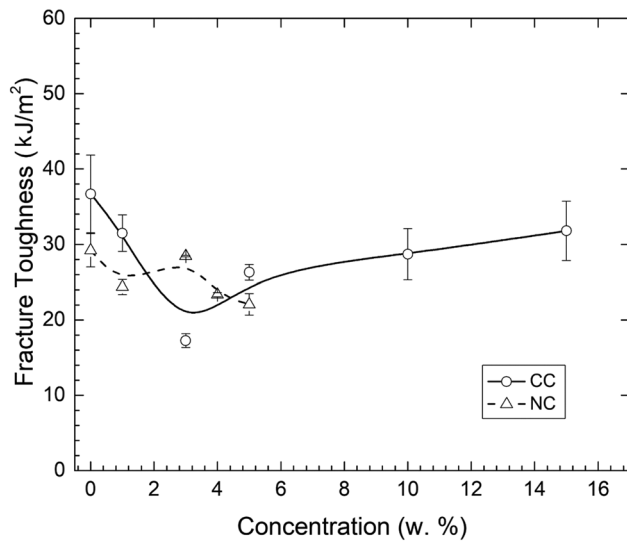
Figure 6: Fracture toughness and filler concentration dependencies of the CC/HDPE and NC/HDPE composites as obtained with Charpy impact testing.

Table 3: Total SFEs and their components (polar and dispersive) of the studied HDPE composites calculated by Owens, Wendt, Rabel, and Kaelble approach from contact angle measurements performed by means of the axisymmetric drop shape analysis (measured at 23°C temperature)

Sample	SFE (mJ/m^2)		
	Total	**Polar**	**Dispersive**
HDPE	19.48 ± 2.91	15.29 ± 2.10	4.19 ± 0.81
CC_1%	36.51 ± 33.80	15.61 ± 14.82	15.61 ± 14.82
CC_3%	36.49 ± 14.86	11.84 ± 7.77	24.65 ± 7.08
CC_5%	39.70 ± 1.09	0.19 ± 0.46	39.51 ± 0.63
CC_10%	23.45 ± 4.41	0.01 ± 0.07	23.44 ± 4.34
CC_15%	26.19 ± 0.05	0.41 ± 0.01	25.78 ± 0.03
NC_1%	30.44 ± 1.04	0.12 ± 0.04	30.32 ± 1.00
NC_2%	30.28 ± 0.92	1.19 ± 0.15	29.09 ± 0.76
NC_3%	32.95 ± 2.58	00.08 ± 0.16	32.86 ± 2.42
NC_4%	29.22 ± 0.66	0.22 ± 0.13	29.00 ± 0.53
NC_5%	23.45 ± 4.41	0.01 ± 0.07	23.44 ± 4.34

steady increase in the modulus of elasticity of polymer-based composites with increasing filler content [21,22].

Upper yield vs filler concentration dependencies of the HDPE composites are shown in Figure 4. They are typical non-linear patterns for both fillers under study (nanoclay and nano calcium carbonate). However, in the case of CC/HDPE composites, the significant changes in the upper yield with increasing filler concentration were not observed with the exception of the composites with 4 and 5 wt% filler concentration for the 200 mm/min deformation rate, where the original values of 25.6 ± 0.4
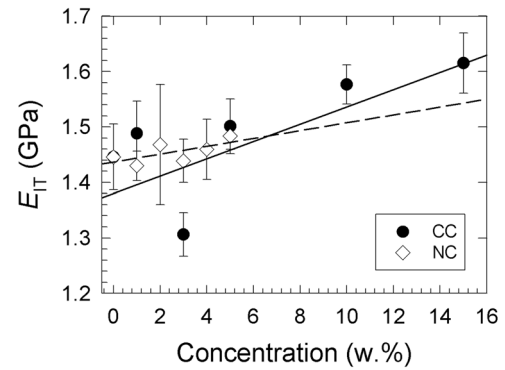

Figure 7: Indentation modulus (EIT) vs filler concentration dependencies. Filler type: full circle – Nano CaCO$_3$ and empty diamond – Nanoclay. *Point omitted for linear regression.

MPa were increasing up to 26.3 ± 0.7 MPa and up to 28.1 ± 2.8 MPa, respectively.

The results of the filler concentration strain at break dependencies measured at different deformation rates are shown in Figure 5. In the case of CC/HDPE composites, observed trend was such that the strain at break was decreased with increasing filler concentration, thus reflecting the loss of plastic behavior, indicating more brittle-like mechanical behavior. This fact fits very well with the well-known theory that polymers with higher crystallinity exhibit higher elastic properties than amorphous systems, which exhibit more plastic behavior [22]. However, the opposite trend was observed for the NC/HDPE composites, where the increased strain at break with increasing filler concentration was found. This was most probably due to the preferential orientation of the individual platelet shape like nanoclay filler particles in the polymer macromolecular chains interphase induced during sample injection molding processing [20]. The comparison of the obtained magnitudes of the elongation at break parameter for 5 wt% nanocomposite filler concentrations (both the nano-clay as well as of the nano-calcium carbonate) confirmed higher plasticity of the composite matrix composed from the nanoclay flat like filler particles for all applied deformation rates. This finding was also in agreement with the mutual comparison of the observed magnitudes of the Young's modulus of elasticity, where the CC/HDPE samples exhibited higher modulus of elasticity than the NC/HDPE samples.

Observed fracture toughness vs filler concentration dependencies of the tested composites are shown in Figure 6. A decrease in the fracture toughness was found for all the composites studied in comparison with the virgin polymer (HDPE). The most significant decrease of about 52.96% was found for the composites containing nano CaCO$_3$ of 3 wt% filler concentration. For NC/HDPE composites, the observed fracture toughness was decreased

to 22.06 ± 1.42 kJ/m^2 magnitude, which was about 39.87% decrease compared to the virgin HDPE. These results clearly demonstrate the higher brittle character of the composites in comparison to the virgin HDPE.

It was found by DSC thermal analysis that the HDPE filled with nano CaCO$_3$ exhibited higher thermal stability in comparison with the virgin HDPE as reflected by increasing T_g from 103.9°C (virgin HDPE) to 126.6°C for 15 wt% CC/HDPE composites. These results were in excellent agreement with the published data of Viljoen and Labuschagné [23]. Similarly, the T_g increased with increasing nano-clay content in the nano-clay/HDPE composites to 128.2°C, thus confirming that the fillers enhanced interaction with the base HDPE matrix.

Results of the SFE calculations are given in Table 3. Obtained results indicated that both fillers (CaCO$_3$ as well as nanoclay) contributed to the observed decrease in the originally more polar character of the virgin HDPE to less polar one as indicated by the observed increase in the dispersive part of SFE from 4.19 ± 0.81 mJ/m^2 (virgin HDPE) to 39.51 ± 0.63 mJ/m^2 (5 wt% CC/HDPE composites) and to 32.86 ± 2.42 mJ/m^2 (3 wt% NC/HDPE composites). The magnitude of the total SFE was increased from 19.48 ± 2.91 mJ/m^2 (virgin HDPE) by about 103.8% up to 39.70 ± 1.09 mJ/m^2 (5 wt% CC/HDPE composites) and by about 69.18% up to 32.95 ± 2.58 mJ/m^2 (3 wt% NC/HDPE composite). Observed results indicate further improvement in the composites interface's adhesive properties, for example, suitable for coating or adhesive joints technical applications.

The composites micro-indentation testing results are shown in Figure 7 where indentation modulus E_{IT} vs filler concentration patterns are shown. These were characteristic with the gradual increase in the indentation modulus with increasing concentrations of both fillers, confirming the fortification effect of the fillers on the mechanical properties of the tested samples.

5 Conclusion

Two different nano-sized mineral fillers (nano CaCO$_3$ and nanoclay) were used in the HDPE composites pilot plant production. The structural as well as mechanical properties of the prepared composites were studied. The fortifying effect of the fillers on the polymer composite's mechanical performance was confirmed as indicated by the increased elastic modulus and the indentation modulus. For example, the absolute value of the modulus of elasticity 970.1 ± 111.7 MPa for original HDPE was increased by about 51.5% to 1470.0 ± 54.7 MPa in the case of nano CC/HDPE composites with 5 wt% filler concentration. For the NC/HDPE composites, the modulus of elasticity was increased by about 34.5% to the absolute value of 1304.9 ± 83.7 MPa with 4 wt% of filler concentration. Additionally, there was confirmed possible modulation of the plastic-elastic mechanical behavior by the type of the filler as well as its concentration used in the final composites testing articles, as confirmed by the increased stress plateau draw region that occurred during the tensile testing and decreased elongation at break with increasing filler concentration. From the practical point of view, the 5 wt% filler concentration seems to be the most favorable one for both CC/HDPE as well as nano-clay/HDPE composites. Simultaneously, the higher thermal stability was found for both nanocomposites in comparison to the virgin HDPE, thus confirming that the fillers enhanced interaction with the HDPE matrix. Based on the abovementioned conclusions, it seems to be advantageous for the application of the latter nanocomposites as the structural elements in the complex product designs offering combined elasto-plastic mechanical behavior in the relatively wide deformation rates regimes accompanied with the higher thermal stability.

Author contributions: All authors have accepted responsibility for the entire content of this manuscript and approved its submission.

Conflict of interest: The authors state no conflict of interest.

References

[1] Lapčík L, Ruszala MJA, Vašina M, Lapčíková B, Vlček J, Rowson NA, et al. Hollow spheres as nanocomposite fillers for aerospace and automotive composite materials applications. Compos B Eng. 2016;106:74–80.

[2] Lapcik L, Vasina M, Lapcikova B, Hui D, Otyepkova E, Greenwood RW, et al. Material characterization of advanced fillers for composites engineering applications. Nanotechnol Rev. 2019;8:503–12.

[3]   Lapcik L, Vasina M, Lapcikova B, Otyepkova E, Waters KE. Investigation of advanced mica powder nanocomposite filler materials: surface energy analysis, powder rheology and sound absorption performance. Compos B Eng. 2015;77:304–10.

[4]   Lapcik L, Vasina M, Lapcikova B, Stanek M, Ovsik M, Murtaja Y. Study of the material engineering properties of high-density poly(ethylene)/perlite nanocomposite materials. Nanotechnol Rev. 2020;9:1491–9.

[5]   Huang X, Zeng L, Li R, Xi Z, Li Y. Manipulating conductive network formation via 3D T-ZnO: a facile approach for a CNT-reinforced nanocomposite. Nanotechnol Rev. 2020;9:534–42.

[6]   Ali SFA, Elsad RA, Mansour SA. Enhancing the dielectric properties of compatibilized high-density polyethylene/calcium carbonate nanocomposites using high-density polyethylene-g-maleic anhydride. Polym Bull. 2021;78:1393–405.

[7]   Drozdov AD, Christiansen Jd. Thermo-viscoelastic and visco-plastic behavior of high-density polyethylene. Int J Solids Struct. 2008;45:4274–88.

[8]   Abareshi M, Zebarjad SM, Goharshadi EK. Effect of milling time and clay content on the thermal stability of polyethylene-clay nanocomposite. J Vinyl Addit Technol. 2016;22:285–92.

[9]   Said M, Seif S, Challita G. Development of blown film linear low-density polyethylene-clay nanocomposites: Part A: manufacturing process and morphology. J Appl Polym Sci. 2020;137:48589.

[10] Escocio VA, Visconte LLY, da Silva Nazareth AL, de Sousa AMF, Pacheco EB. Permeability, melt flow index, mechanical, and morphological properties of green HDPE composites: effect of mineral fillers. Macromolecular symposia. Vol. 381. Weinheim: Wiley-VCH GmbH; 2018. UNSP 1800127.

[11] Chan JX, Wong JF, Hassan A, Mohamad Z, Othman N. Mechanical properties of wollastonite reinforced thermoplastic composites: a review. Polym Compos. 2020;41:395–429.

[12] Sepet H, Aydemir B, Tarakcioglu N. Evaluation of mechanical and thermal properties and creep behavior of micro-and nano-CaCO(3) particle-filled HDPE nano- and microcomposites produced in large scale. Polym Bull. 2020;77:3677–95.

[13] Se pet H, Tarakcioglu N, Misra RDK. Investigation of mechanical, thermal and surface properties of nanoclay/HDPE nanocomposites produced industrially by melt mixing approach. J Composite Mater. 2016;50:3105–16.

[14] Sepetcioglu H. The effect of nanoclay on the nonlinear viscoelastic behavior of high-density polyethylene. Polym Compos. 2021;42:3481.

[15] Sepet H, Tarakcioglu N, Misra RDK. Determination of the mechanical, thermal and physical properties of nano-CaCO$_3$ filled high-density polyethylene nanocomposites produced in an industrial scale. J Composite Mater. 2016;50:3445–56.

[16] Kwok D. The usefulness of the Lifshitz-van der Waals/acid-base approach for surface tension components and interfacial tensions. Colloid Surf A-Physicochem Eng Asp. 1999;156:191–200.

[17] Gajdosikova R, Lapcikova B, Lapcik L. Surface phenomena and wetting of porous solids. Phys Chem: Indian J. 2011;6:146–62.

[18] Oliver W, Pharr G. Measurement of hardness and elastic modulus by instrumented indentation: advances in understanding and refinements to methodology. J Mater Res. 2004;19:3–20.

[19] Manas D, Mizera A, Manas M, Ovsik M, Hylova L, Sehnalek S, et al. Mechanical properties changes of irradiated thermoplastic elastomer. Polymers. 2018;10:87.

[20] Lapcik L, Manas D, Lapcikova B, Vasina M, Stanek M, Cepe K, et al. Effect of filler particle shape on plastic-elastic mechanical behavior of high density poly(ethylene)/mica and poly(ethylene)/wollastonite composites. Compos Pt B-Eng. 2018;141:92–9.

[21] Lapčík L, Maňas D, Vašina M, Lapčíková B, Řezníček M, Zádrapa P. High density poly(ethylene)/CaCO$_3$ hollow spheres composites for technical applications. Compos Pt B-Eng. 2017;113:218–24.

[22] Bucknall CB. Toughened plastics. Dordrecht: Springer Science + Business Media, B.V.; 1977.

[23] Viljoen WD, Labuschagne FJWJ. The thermal stability of highly filled high-density polyethylene quaternary composites: interactive effects and improved measures. Polym Test. 2020;85:106424.